Lack of secondary structure characterizes the 5′ ends of mammalian mitochondrial mRNAs

CHRISTIE N. JONES, KEVIN A. WILKINSON, KIMBERLY T. HUNG,[1] KEVIN M. WEEKS, and LINDA L. SPREMULLI

Department of Chemistry, University of North Carolina at Chapel Hill, Chapel Hill, North Carolina 27599-3290, USA

ABSTRACT

The mammalian mitochondrial genome encodes 13 proteins, which are synthesized at the direction of nine monocistronic and two dicistronic mRNAs. These mRNAs lack both 5′ and 3′ untranslated regions. The mechanism by which the specialized mitochondrial translational apparatus locates start codons and initiates translation of these leaderless mRNAs is currently unknown. To better understand this mechanism, the secondary structures near the start codons of all 13 open reading frames have been analyzed using RNA SHAPE chemistry. The extent of structure in these mRNAs as assessed experimentally is distinctly lower than would be predicted by current algorithms based on free energy minimization alone. We find that the 5′ ends of all mitochondrial mRNAs are highly unstructured. The first 35 nucleotides for all mitochondrial mRNAs form structures with free energies less favorable than −3 kcal/mol, equal to or less than a single typical base pair. The start codons, which lie at the very 5′ ends of these mRNAs, are accessible within single stranded motifs in all cases, making them potentially poised for ribosome binding. These data are consistent with a model in which the specialized mitochondrial ribosome preferentially allows passage of unstructured 5′ sequences into the mRNA entrance site to participate in translation initiation.

Keywords: mitochondria; mRNA; translation initiation; RNA SHAPE chemistry

INTRODUCTION

Mammalian mitochondria contain a double stranded genome of ~16 kilobase pairs (Anderson et al. 1981, 1982). Encoded within the genome are 13 membrane proteins that function in the electron transfer chain or are components of the ATP synthase complex. The 13 mitochondrially encoded proteins are translated from 9 monocistronic and 2 dicistronic mRNAs. Both dicistronic mRNAs contain overlapping reading frames (Fig. 1A; Anderson et al. 1981, 1982). With the exception of the two internal start sites found in the dicistronic mRNAs, the remaining 11 start sites are located at or near the 5′ end of each mRNA (Montoya et al. 1981). These mRNAs therefore have no 5′ untranslated region and are leaderless. These leaderless mRNAs are translated by the specialized protein biosynthetic system found in mitochondria. The start codon at the 5′ end can be either AUG or AUA, both of which encode methionine in mammalian mitochondria. These codons direct the insertion of formylmethionine during initiation and methionine during chain elongation. In bovine mitochondria, AUG serves as the start codon for 10 genes while AUA is used for the remaining three genes.

An early and fundamental step in protein synthesis is recognition of the start codon in the mRNA by the ribosomal small subunit. This process is achieved by different, well-established mechanisms in prokaryotes and for nuclear encoded genes in eukaryotes. In prokaryotes, most mRNAs have an untranslated region upstream of the start codon that contains the Shine–Dalgarno (SD) sequence. This sequence base pairs with the anti-SD sequence in the 16S rRNA of the 30S subunit and positions the mRNA start codon at the P-site of the ribosome (Shine and Dalgarno 1974; Gualerzi et al. 2000). In addition to the simple presence of the SD sequence, the physical accessibility of the SD sequence and its associated start codon is a major determinant for translational initiation in prokaryotes (Boni 2006; Nakamoto 2006). The underlying secondary structure of the mRNA can function to prevent initiation at incorrect methionine codons and to facilitate the recognition of the

[1]**Present Address:** Division of Cancer Genetics and Epidemiology, Lombardi Cancer Center, Georgetown University Medical Center, Washington, DC 20057, USA.

Reprint requests to: Linda L. Spremulli, Department of Chemistry, Campus Box 3290, University of North Carolina at Chapel Hill, Chapel Hill, NC 27599-3290, USA; e-mail: Linda_Spremulli@unc.edu; fax: (919) 843-1580; or Kevin M. Weeks, Department of Chemistry, Campus Box 3290, University of North Carolina at Chapel Hill, Chapel Hill, NC 27599-3290, USA; e-mail: Weeks@unc.edu; fax: (919) 962-2388.

Article published online ahead of print. Article and publication date are at http://www.rnajournal.org/cgi/doi/10.1261/rna.909208.

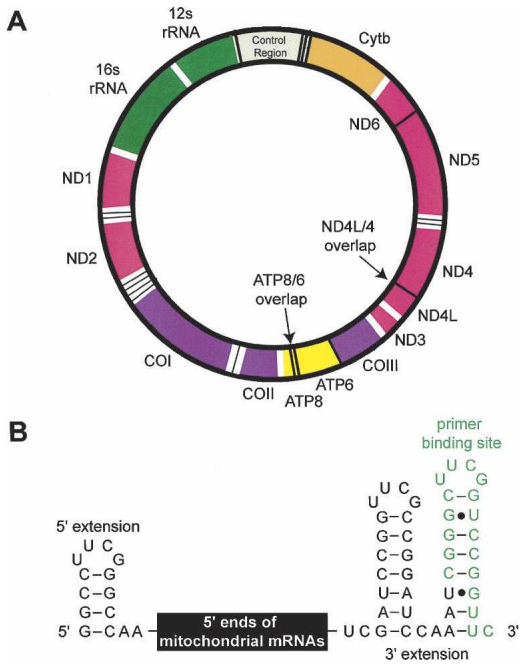

FIGURE 1. The mitochondrial genome and strategy for analyzing the 5′ ends of mitochondrial mRNAs. (*A*) The mammalian mitochondrial genome encodes 13 proteins, each of which is a subunit of the oxidative phosphorylation machinery. Protein coding genes and the two overlapping dicistronic mRNAs are shown explicitly. The protein encoding genes are generally separated by one or more tRNA genes (white); noncoding rRNA genes are green. (*B*) Messenger RNA fragments used for SHAPE analysis. The 5′ and 3′ extensions facilitate structural analysis of the 5′ end of the mRNA sequence and provide an efficient reverse transcriptase primer binding site, respectively.

correct initiation codon (Boni 2006; Nakamoto 2006). Translational initiation in eukaryotes functions by a different mechanism. Eukaryotic mRNAs contain a cotranscriptionally added 7-methylguanosine triphosphate cap at their 5′ ends and are post-transcriptionally polyadenylated at their 3′ ends (Sachs et al. 1997). Eukaryotic initiation factors bind the 5′ cap and 3′ poly(A) tail and provide a platform for binding by the small 40S ribosomal subunit (Kapp and Lorsch 2004). Once bound, the small subunit scans the mRNA in the 5′ to 3′ direction to locate the start codon.

In contrast to these well-developed models, the mechanism by which the translational start codon is recognized in mammalian mitochondria is unknown. Mammalian mitochondrial mRNAs do not have a SD sequence upstream of the start codon nor does the small subunit (28S) ribosomal RNA (12S rRNA) contain an anti-SD sequence (Anderson et al. 1982). These mRNAs also lack a 5′ cap and thus resemble the rare leaderless mRNAs found in prokaryotes. Leaderless mRNAs in prokaryotes may actually be initiated on 70S ribosomes rather than on the 30S subunit (Moll et al. 2004; Udagawa et al. 2004).

The fact that mitochondrial mRNAs are leaderless raises the question of whether information exists at or near the 5′ ends of these RNAs that enables them to be efficiently recognized by the mitochondrial translational machinery. No in vitro translational system that might allow a direct test of this question has been established for mammalian mitochondria, nor have any additional protein factors that function in start site selection been identified. It is therefore possible that the structure of the mRNA alone guides the ribosome to the proper start codon. This guiding or recognition function could be achieved by a conserved structural element detected by the ribosome. Alternatively, it could be based on the unique accessibility of the start codon at the 5′ end of the mRNA. To begin to address these models, we have analyzed the secondary structure at the 5′ ends of all 13 protein coding regions in the bovine mitochondrial transcriptome at single nucleotide resolution using RNA SHAPE chemistry. Secondary structure predictions based on thermodynamic free energy minimization calculations indicate that the 5′ ends of many mitochondrial mRNAs can, in principle, form short, stable secondary structures. In contrast to predictions based on free energy parameters alone, when experimental SHAPE information is used to constrain secondary structure predictions, we find that the 5′ ends of bovine mitochondrial mRNAs show a strong propensity to be highly unstructured. Our analysis indicates that the start codon tends to lie in a single-stranded region or in a very weak duplex stem. These data support a model in which translational initiation in mitochondria is not guided by a conserved secondary structural element but, instead, that the mitochondrial ribosome recognizes structurally accessible and single stranded start codons.

RESULTS

Strategy

To investigate the structure near the 5′ ends of mitochondrial mRNAs, RNA constructs containing approximately the first 70 nucleotides (nt) of each mRNA were prepared. The selected region of each mRNA was flanked on the 5′ end by an extension allowing structural analysis to include the entire 5′ end of the mRNA (Fig. 1B). On the 3′ end, the mRNA carried an extension that contained a strong primer binding site to ensure uniform reverse transcription (Wilkinson et al. 2005). The structure formed by the first ~70 nt of each of the mRNAs was then analyzed using RNA SHAPE chemistry (Wilkinson et al. 2006).

In a SHAPE experiment, local nucleotide flexibility is detected as the preferential ability of the 2′-hydroxyl group of nucleotides at conformationally dynamic sites to react with an electrophile to form a 2′-O-adduct. The structure of each RNA was assessed by treating the RNA with N-methylisatoic anhydride (NMIA). Background was analyzed in a mock reaction omitting the reagent, performed in parallel. Sites of 2′-O-adduct formation were detected by primer extension. Two dideoxy sequencing reactions were

also performed in parallel to yield a sequencing ladder allowing identification of modified sites. The SHAPE extension reactions and sequencing ladders were resolved on a sequencing gel. The relative reactivities of each nucleotide were used as constraints in conjunction with structure prediction based on free energy minimization (Mathews et al. 2004) to generate secondary structure models satisfying the imposed SHAPE constraints. We will focus on the analysis of three mitochondrial messages in detail (ND2, COIII, and COII) and then summarize the experimentally supported structures for all 13 mRNAs (see Fig. 1A).

NADH dehydrogenase subunit 2 (ND2) mRNA

Of the 13 protein-coding sequences in the mitochondrial genome, seven open reading frames encode subunits of the NADH dehydrogenase complex (Complex I). Five of these are encoded as monocistronic mRNAs, while 2 are encoded in the form of the dicistronic ND4/4L transcript (Taanman 1999).

In one representative example, we analyzed a 78-nt fragment of the ND2 mRNA using RNA SHAPE chemistry (Fig. 2). The RNA was folded in the presence of Mg^{2+} and subsequently treated with NMIA to assess local RNA structure or subjected to a mock reaction omitting the reagent to assess background. There were no significant stops in the control experiment omitting NMIA. In contrast, the RNA was highly modified upon treatment with the reagent (Fig. 2A, cf. "+" and "−" NMIA lanes). Reactivities were normalized to a scale spanning 0 to ~1.2 in which the average intensity of highly reactive positions was defined as having a reactivity of 1.0 (Wilkinson et al. 2006). SHAPE reactivities can vary continuously from 0 to 1.2. To simplify visual analysis of this information, positions with high and medium reactivities will be colored red and yellow, respectively. Residues with little or no reactivity will be black.

Most nucleotides between positions 1 and 45 in the ND2 mRNA are highly susceptible to modification, indicating that a considerable portion of this RNA is flexible and, consequently, has little or no secondary or tertiary structure. While most nucleotides in this RNA are highly modified, nucleotides 46–56, 61–65, and 67–72 are unreactive toward NMIA (Fig. 2B). We used the experimental SHAPE reactivities to predict a secondary structure for this RNA (Fig. 2C). The predicted structure contains a single

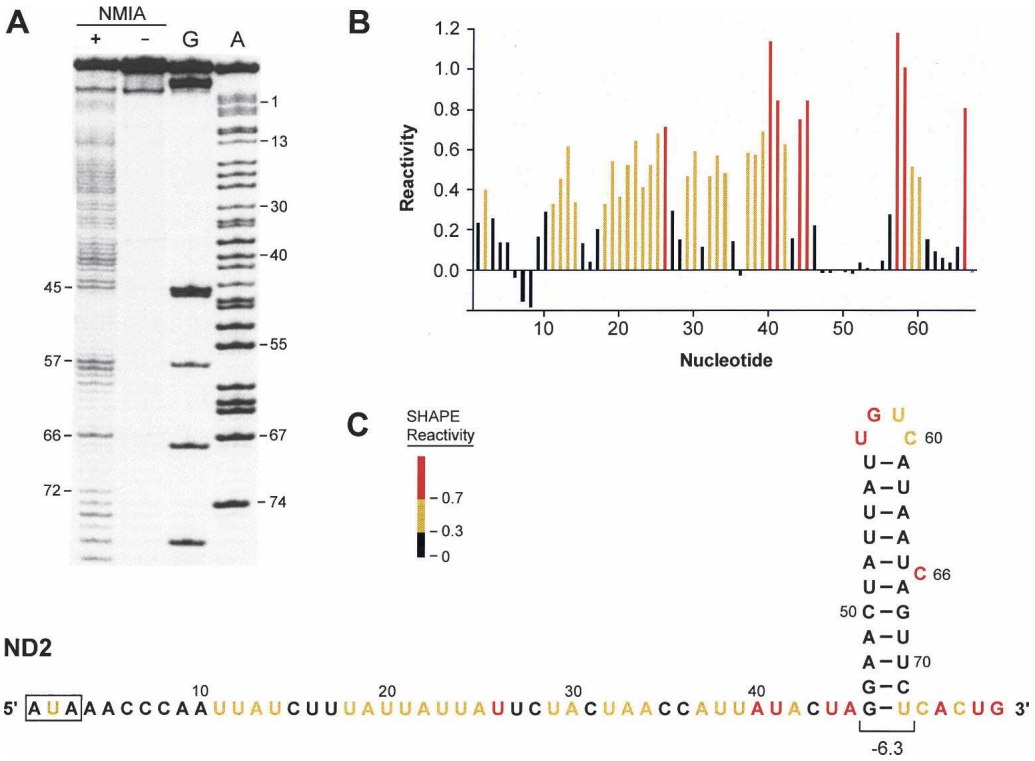

FIGURE 2. SHAPE analysis of the 5′ end of the ND2 mRNA. (*A*) Gel image showing the NMIA modification reaction (+), the no reagent control (−), and G and A dideoxy sequencing ladders. (*B*) Histogram of normalized SHAPE reactivities after correcting for drop off. The histogram bar colors correspond to SHAPE reactivities. Nucleotides are defined as having a high reactivity (red), moderate reactivity (yellow), or low reactivity (black). (*C*) Predicted secondary structure for the 5′ end of the ND2 mRNA as constrained by SHAPE reactivities. Nucleotide colors correspond to those in panel *B*. The reactivities for nucleotides 68–73 were assigned by visual analysis of the gel. Although the first 10 nt of this RNA have low (but still significant) reactivities, there are no obvious pairing partners for these positions in the RNA and flanking structure cassette. These nucleotides are thus predicted to be single stranded.

hairpin with a C bulge. The calculated free energy of this stem–loop is −6.3 kcal/mol (Fig. 2C). The SHAPE reactivities exactly match the predicted structure because unmodified nucleotides lie in the hairpin stem, while the single nucleotide bulge at position 66 is reactive. The remainder of this mRNA, including the AUA start codon, is predicted to be unstructured.

These data emphasize the high degree of structural detail that can be obtained in a SHAPE analysis. Even though mitochondrial mRNAs contain a low fraction of guanine residues, it is still possible for these RNAs to form stable secondary structures as evidenced by the stem–loop at positions 46–72 in the ND2 message. This well-defined stable structure stands in strong contrast to the first 45 nt in the ND2 message, which are highly flexible and do not form a stable secondary structure (Fig. 2C).

Cytochrome oxidase subunit II and III mRNAs

Three subunits of cytochrome oxidase (CO) (Complex IV) in the oxidative phosphorylation pathway are encoded within the mitochondrial genome (COI, COII, and COIII). The mRNA for the 30-kDa COIII subunit is 781 nt in length and begins with an AUG start codon. We used SHAPE chemistry to analyze a 5′ fragment of the COIII RNA in the context of the 5′ and 3′ extensions of the structure cassette. To address the general possibility that the 5′ extension might affect the structure of the internal mRNA, we analyzed the same COIII RNA fragment lacking the 5′ extension. Comparison of the reactivity profiles revealed that the 5′ extension had no significant effect on nucleotide reactivity (Fig. 3A, see "+" NMIA lanes in the extension and no 5′ extension lanes). A comparison of the integrated SHAPE intensities shows that the reactivities for the two RNAs are essentially identical (Fig. 3B, blue and green bars) In both cases, the 5′ end of the RNA is predicted to form the same structure (Fig. 3C). This structure contains a set of two stem–loops, with the potential to stack coaxially. However, these structures are just barely stable and have a net free energy of formation of −0.7 and −0.3 kcal/mol. It is likely that there are multiple weak structures in equilibrium. The AUG start codon at the 5′ end is

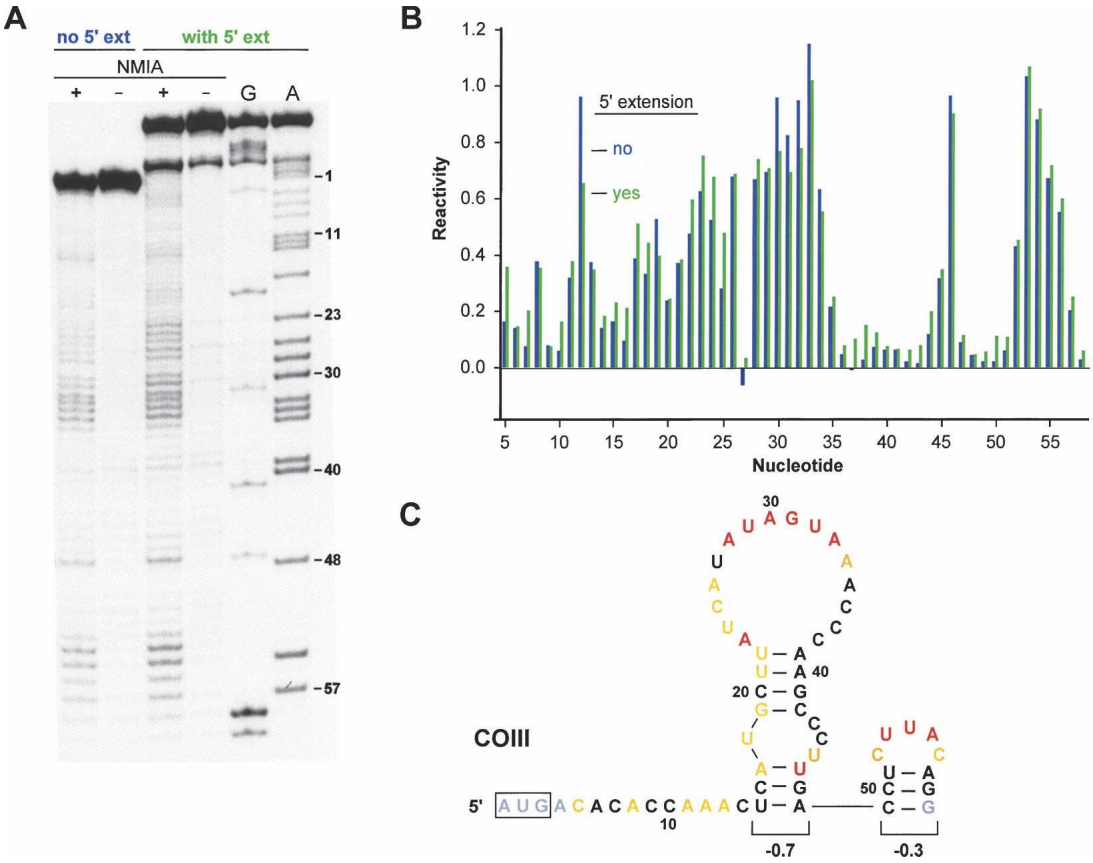

FIGURE 3. SHAPE analysis of the 5′ end of the COIII mRNA. Panels *A*–*C* were generated as described for Figure 2 with the following additions. (*A*) Gel image showing sites of 2′-O-adduct formation for the COIII mRNA fragment both with and without the 5′ extension from the structure cassette. G and A sequencing ladders correspond to the COIII RNA containing the 5′ extension. (*B*) Absolute SHAPE reactivities. Histograms for the COIII mRNA fragment without and with the 5′ extension are blue and green, respectively. (*C*) Secondary structure model for the COIII mRNA fragment. Positions for which no data were obtained are gray. Identical structures are predicted for the RNAs without and with the 5′ extension.

predicted to be fully unpaired. These experiments emphasize that the structure cassette does not affect the folding of the internal mRNA sequence and that the 5′ end of the COIII mRNA lacks significant structure.

The mRNA for cytochrome oxidase subunit II (COII) is 684-nt long and begins with an AUG start codon. For this RNA, we addressed the question of whether the structure of a 5′ fragment is a good model for the structure of the full mRNA. Hence, for this RNA, we analyzed both a 5′ fragment and an RNA spanning the full 684 nt of the mRNA. This analysis allows us to assess whether long-range pairings might be prevalent and affect the SHAPE profile at the 5′ ends of these RNAs. For both RNAs, SHAPE chemistry was performed under identical conditions and the sites of modification were analyzed using an internal DNA primer complementary to COII nucleotides 64–82 (Fig. 4A, cf. "fragment" and "full length" lanes). The two RNAs have very similar SHAPE reactivity patterns (Fig. 4B, cf. blue and green bars in the histogram). Both reactivity patterns also support essentially the same structure for the 5′ end of this RNA with one minor difference. The full-length data support a slightly less stable structure in which the U-A pair at the base of the stem (shown in Fig. 3C) does not form. The overall secondary structure features a single stem–loop, interrupted by an internal loop that partially incorporates the AUG start codon (Fig. 4C). Although the stem–loop structure spans 28 nt, its overall stability is still low and has a total free energy of only −3.2 kcal/mol. This analysis supports the conclusion that the ~70 nt at the 5′ end of the mRNA yield a SHAPE profile and overall structure that is representative of the full-length mRNA.

Other monocistronic mRNAs

We analyzed 5′ RNA fragments for the other six monocistronic mRNAs in mammalian mitochondria. These included the remaining subunit of the cytochrome oxidase complex (COI) (Fig. 5A); the other four subunits of the NADH dehydrogenase complex (Fig. 5B–E); and of cytochrome b (Cytb), which is the only subunit of complex III of the electron transfer chain encoded in the mitochondrial genome (Fig. 5F). Strikingly, SHAPE analysis reveals that all of these RNAs are largely unstructured (Fig. 5, note yellow and red nucleotides). The most stable single secondary structural element is found in the COI RNA and consists of a reasonably stable stem–loop whose formation is 4.2 kcal/mol more stable than the corresponding single strand (Fig. 5A). Note that this stable stem lies 39 nt from the

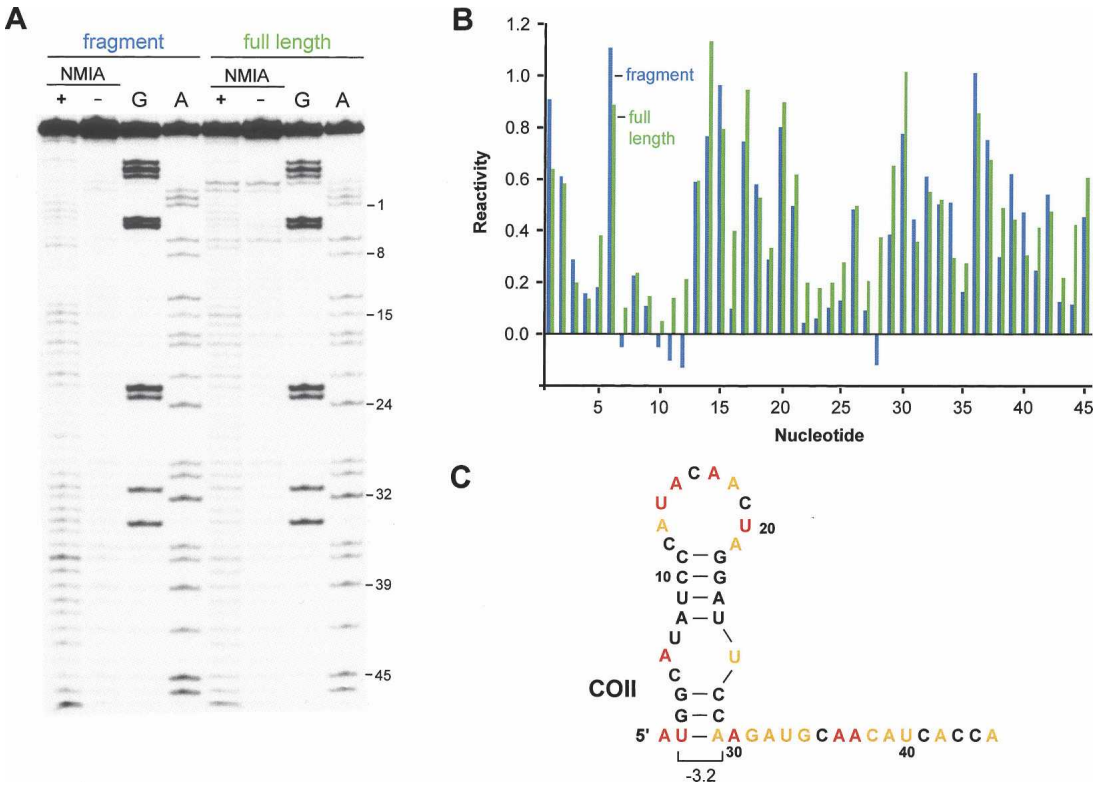

FIGURE 4. SHAPE analysis of the 5′ end of the COII mRNA. Panels *A–C* were generated as described for Figure 2 with the following additions. (*A*) Gel image shows sites of 2′-O-adduct formation for the 82-nt-long COII fragment and for the full-length mRNA. (*B*) Histograms for the COII fragment and full-length mRNA reactivities are in blue and green, respectively. (*C*) Secondary structure model for the COII mRNA fragment.

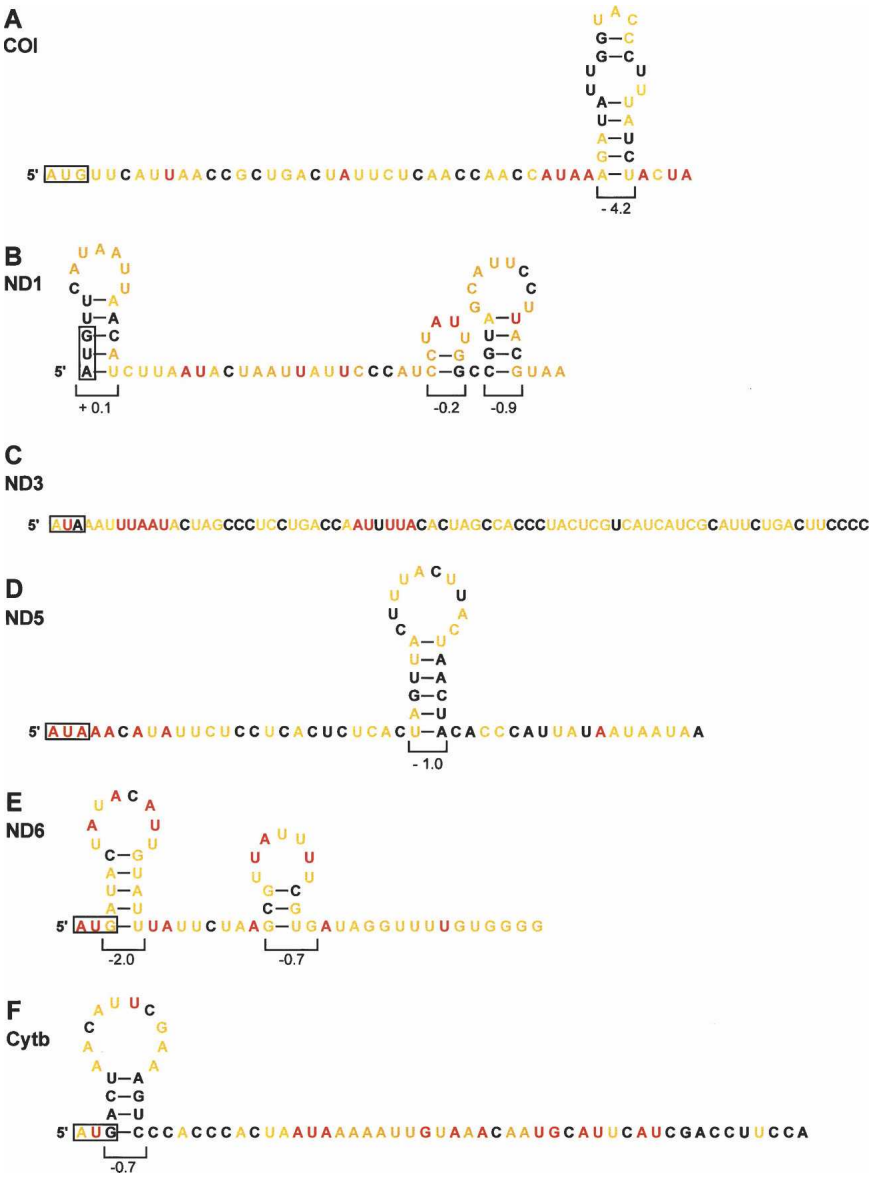

FIGURE 5. SHAPE-supported secondary structure models for the 5′ ends of the COI, ND1, ND3, ND5, ND6, and Cytb mRNAs. Nucleotides are colored by reactivity using the scheme shown in Figure 2. Calculated stabilities (Mathews et al. 2004) for individual stable stem–loop structures (in kcal/mol) are indicated. Start codons are boxed.

5′ end of this RNA such that the AUG start site is still in a conformationally flexible region (Fig. 5A). The 5′ regions of the remaining mRNAs are predicted to be essentially unstructured. For completeness, the most stable secondary structure for each RNA is shown in Figure 5, and none of these has a stability greater than 2.0 kcal/mol, a free energy increment equivalent to a single A-U base pair (Mathews et al. 1999).

Dicistronic mRNAs

There are two dicistronic mRNAs in mammalian mitochondria. One of these encodes the ND4L and ND4 proteins, both subunits of Complex I. This mRNA initially codes for ND4L. The reading frames for the two proteins overlap such that the AUG start codon of ND4 is 1 nt upstream of the stop codon for ND4L (Fig. 6B). The second dicistronic mRNA encodes ATPase subunit 8 (ATP8) as the first cistron and ATPase subunit 6 (ATP6) as the second cistron. Both of these subunits are components of mitochondrial Complex V (the ATP synthase). The reading frames for these proteins overlap by 40 nt (Fig. 6D).

The 5′ end fragments of both dicistronic mRNAs (corresponding to synthesis of ND4L and ATP8) were analyzed by SHAPE. Both RNAs have the ability to form single stem–loop structures (Fig. 6A,C); however, neither is more stable than a single G-C base pair (stabilities are −0.1 and −2.7 kcal/mol, respectively). The start codon for both ND4L and ATP8 lie in very weakly or unstructured regions that would be readily accessible to the ribosome. Thus, the 5′ ends of the two dicistronic messages conform to the pattern identified for the monocistronic messages (Figs. 2C, 3C, 4C, 5) and have no stable secondary structural elements near the 5′ start codons.

We next analyzed fragments containing the overlapping coding regions for the ND4L/ND4 and ATP8/ATP6 messages, which spanned 88 and 92 nt, respectively (Fig. 6B,D). The start codon of ND4 and the stop codon of ND4L both lie in highly unstructured regions and both are predicted to be single stranded. Moreover, these codons lie in a large unstructured domain. We speculate that the initiation of translation at the ND4 start site occurs by slippage of the ribosome or small subunit from the ND4L stop codon back to the ND4 start codon. However, if de novo initiation occurs, then the lack of structure may be important for facilitating the process.

At the ATP8/ATP6 junction, there is also essentially no significant structure (Fig. 6D). Both the start codon of ATP6 and the stop codon of ATP8 lie in unstructured and likely highly accessible regions. There are 40 nt between the beginning of the start codon of ATP8 and the end of the stop codon of ATP8. Initiation of translation of the ATP6 message may require an independent initiation event, rather than ribosome slippage. An independent initiation event is likely

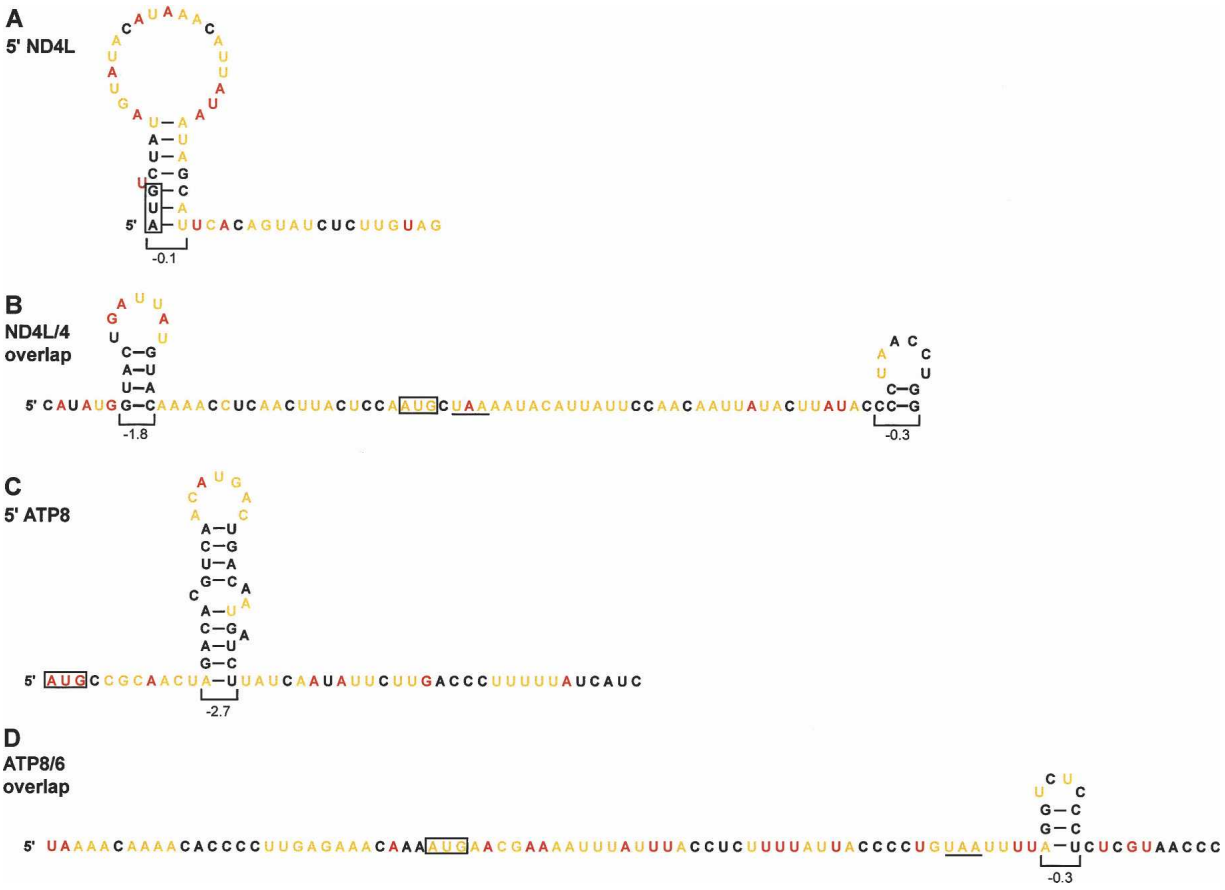

FIGURE 6. Secondary structures at the 5′ translational start sites (*A*,*C*) and at the junctions between coding regions (*B*,*D*) for the dicistronic mRNAs. Start codons are boxed and the stop codons for the first cistrons (ND4L or ATP8) are underlined. Nucleotides are colored by SHAPE reactivity using the color scheme shown in Figure 2.

to be strongly facilitated by the absence of structure in the region. One interesting observation in this case is the absence of AUG or AUA triplets in or around the overlapping reading frames, possibly facilitating correct translational initiation at the ATP6 start site. Interestingly, initiation of these internal messages occurs at the first codon located upstream of the stop codon for the initial message in RNA regions devoid of measurable secondary structure (Fig. 6B,D).

DISCUSSION

mRNA structure in a small transcriptome

We have analyzed the 5′ ends of all translated RNAs in a single, small transcriptome. This analysis reveals that all 11 mRNAs in bovine mitochondria are highly unstructured. Specifically, as judged by SHAPE-constrained secondary structure prediction, there are no structures with a net stability greater than −3 kcal/mol in the first 35 nt of any of these RNAs and, for most mRNAs, no structure forms that has a calculated stability of even −1.0 kcal/mol (Figs. 2C, 3C, 4C, 5, 6).

Mitochondrial genomes tend to be A/U rich, and one explanation for the low extent of secondary structure might simply reflect the lower stability of A-U base pairs as compared with G-C base pairs. However, we find that some mRNA sequences do form stable secondary structures near their 5′ ends: The ND2 and COI messages contain stem-loops with calculated stabilities of −6.3 and −4.2 kcal/mol, respectively (Figs. 2C, 5A). These structures lie 45 and 39 nt from the 5′ ends of their respective mRNAs. Furthermore, the structured mitochondrial tRNAs and rRNAs are also A/U rich, indicating that the high A/U content by itself does not preclude the formation of significant structure. Thus, these data suggest mitochondrial mRNAs have the potential to form stable local structures but that such structures do not form near the 5′ ends of these mRNAs.

Requirement for experimental information in inferring mitochondrial mRNA structure

We also assessed the extent to which the SHAPE reactivity information modulates the predicted secondary structure models for the mitochondrial mRNA leader sequences. In the absence of experimental structural information, the

most stable structure for an RNA can be estimated using thermodynamic parameters based on a dinucleotide sequence model, supplemented by other information for loops and multihelix junctions (Zuker 2003; Eddy 2004; Mathews and Turner 2006). We calculated secondary structures for the 5′ ends of all 11 bovine mitochondrial mRNAs using a well-established thermodynamic model (Mathews et al. 2004). In general, the 5′ ends of these leaderless mRNAs are predicted to contain significant structure, with free energies ranging from −2.0 to −7.1 kcal/mol (Fig. 7).

Comparison of the thermodynamic-only versus SHAPE-constrained predictions reveals that the differences fall into three classes. For three RNAs (ND2, ND5, and COI), the predicted models are identical. For the COIII RNA, there are minor differences between the structural models. In the third class, encompassing seven of the 11 leader sequences, there are large differences between the thermodynamic-only and SHAPE-constrained structures (compare structures in Fig. 7 with those in other figures). The differences between structures show a clear pattern. Structures predicted based on thermodynamic parameters alone contain many more base-paired regions than do the SHAPE-constrained models. In general, the "extra" helical regions tend to involve nucleotides that have high SHAPE reactivities and, thus, are not consistent with direct experimental tests of these structures (see Fig. 7). These data are consistent with the general observation that thermodynamic models alone tend to overpredict secondary structures for RNAs of known structure (Mathews and Turner 2006). Importantly, the clear demonstration that the 5′ leaders of bovine mitochondrial mRNAs are characterized by a lack of stable secondary structure was dependent on having single nucleotide resolution SHAPE information. We hypothesize that the conserved lack of structure at the 5′ ends of mitochondrial mRNAs plays a functional role in mitochondrial translational initiation.

Structural requirements for translation initiation in mammalian mitochondria

Overall, the mechanism of translational initiation for the leaderless mitochondrial mRNAs remains poorly understood. This mechanism is likely to be distinct from initiation of leaderless mRNAs in prokaryotes. In prokaryotes, initiation of leaderless mRNAs is thought to occur on preformed 70S ribosomes rather than on the small subunit, as is the predominant mechanism in the cytoplasm of both prokaryotes and eukaryotes (Gualerzi et al. 2000; Kapp and Lorsch 2004; Udagawa et al. 2004). In the model for leaderless prokaryotic translational initiation, IF2 promotes binding of fMet-tRNA to the intact 70S ribosome instead of to the small 30S ribosomal subunit (Udagawa et al. 2004). In contrast, the presence of an IF3 homolog in mitochondria ($IF3_{mt}$) argues that initiation on mitochondrial mRNAs occurs on 28S subunits. IF3 functions to dissociate intact ribosomes into their constituent subunits, in both the prokaryotic and mitochondrial systems. In prokaryotes, IF3 antagonizes initiation of leaderless mRNAs, which require intact 70S ribosomes (Udagawa et al. 2004), whereas $IF3_{mt}$ stimulates initiation complex formation in the presence of mitochondrial 55S ribosomes (Koc and Spremulli 2002). This stimulation is consistent with the ability of $IF3_{mt}$ to dissociate 55S ribosomes and, thereby, to increase the concentration of initiation-active 28S subunits (Koc and Spremulli 2002).

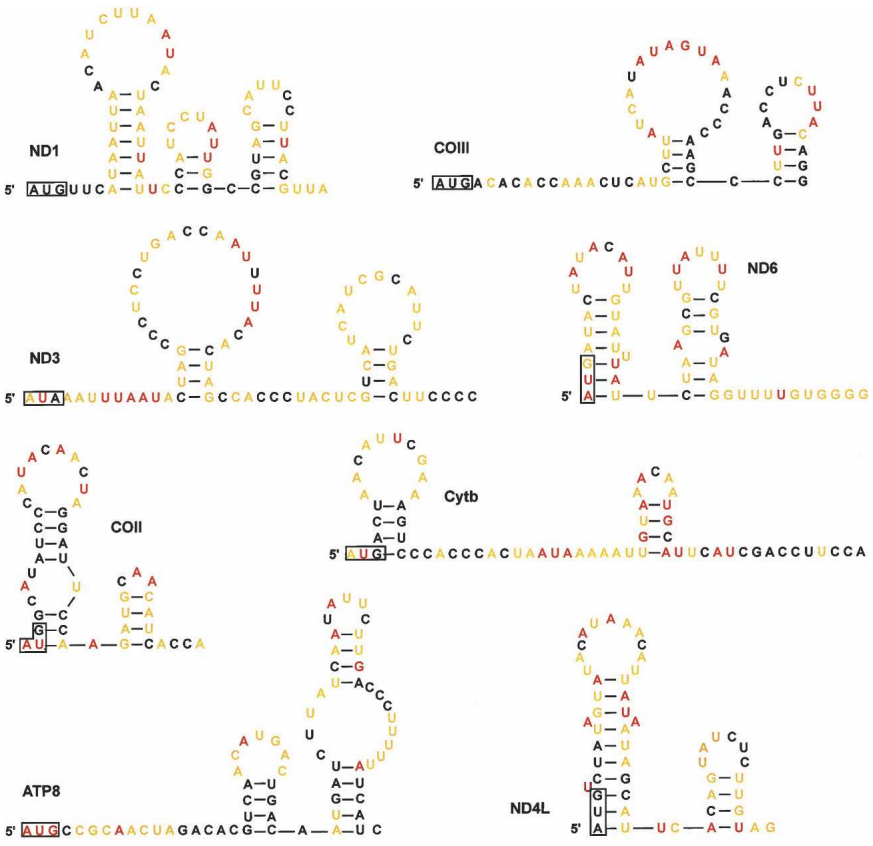

FIGURE 7. Secondary structures for the leaderless mammalian mitochondrial mRNAs predicted without the use of experimental SHAPE information. Structures were predicted using RNAstructure (Mathews et al. 2004). Experimental SHAPE reactivities are superimposed in color using the scheme shown in Figure 2. Only those structures that differ from the SHAPE-constrained structures are shown.

The small ribosomal subunit must then select the correct AUG or AUA start codon. The unifying characteristic among the mitochondrial mRNAs is that the start codon lies exactly at the 5′ end of the message. SHAPE analysis indicates that all start codons in mammalian mitochondrial mRNAs lie in mRNA regions with little or no local structure. It is likely that this structural accessibility is important for providing a suitable platform for the initiating ribosome, as has been suggested for the leaderless mRNAs found in the prokaryotic system (Moll et al. 2002).

One of the most distinctive differences between mitochondrial and bacterial ribosomes is the presence of a triangular gatelike structure at the mRNA entrance site on the small subunit of the mitochondrial ribosome (Sharma et al. 2003). The mRNA gate is formed almost completely by proteins that are specific to the mammalian mitochondrial ribosome. Thus, in the small 11 mRNA transcriptome of bovine mitochondria, both the mRNA start codon and also the mRNA entry site appear to have developed distinctive adaptations. The distinctive mitochondrial mRNA entry gate (Sharma et al. 2003) may function to allow passage of only unstructured mRNA 5′ sequences into the small subunit for subsequent recognition of the start codon and translational initiation.

MATERIALS AND METHODS

Plasmids

The plasmids p11-1 and p11-5 (Hauswirth and Laipis 1982), containing the bovine mitochondrial genome, were kindly provided by Dr. Philip Laipis (University of Florida). The plasmid pTZ19R-CoII containing the bovine mitochondrial cytochrome oxidase subunit II gene was prepared as described (Liao and Spremulli 1989).

RNA synthesis

DNA transcription templates containing the 5′ portion of each mRNA, flanked on either side by a stably folding structural cassette (Merino et al. 2005) were prepared by PCR. Reactions (100 μL) contained 10 mM KCl, 10 mM $(NH_4)_2SO_4$, 20 mM Tris-HCl (pH 8.8), 2 mM $MgSO_4$, 0.1% Triton X-100, 250 μM each dNTP, 1 μM each forward and reverse primer, 15–30 ng linearized pTZ19R-CoII or 150–1200 ng of linearized p11-1 or p11-5 plasmid DNA, and 0.02 units/μL of Vent DNA polymerase (NEB) and were subjected to 33 cycles (denaturation at 95°C for 45 sec; annealing 50–65°C for 30 sec; elongation 72°C for 90 sec). The PCR product was recovered by ethanol precipitation and resuspended in 100 μL water. Transcription reactions (300 μL, 37°C, 4–5 h) contained 40 mM Tris-HCl (pH 7.6), 20 mM $MgCl_2$, 2 mM spermidine, 10 mM dithiothreitol (DTT), 0.1 mg/mL bovine serum albumin, 0.2 U/μL SUPERase•In RNase inhibitor, 4 mM each NTP, 100 μL PCR-generated template, and a saturating amount of T7 RNA polymerase. The RNA product was precipitated with ethanol and resuspended in 100 μL water. The RNA was purified by denaturing (8%) polyacrylamide gel electrophoresis (29:1 acrylamide:bisacrylamide prepared with 7 M urea, 90 mM Tris-borate, 2 mM EDTA), visualized by UV shadowing, excised from the gel, recovered by passive elution in water and ethanol precipitation, and resuspended in 100 μL water.

SHAPE analysis

RNA (4 pmol) in 24 μL water was heated at 95°C for 2 min and then cooled on ice for 2 min. The RNA was treated with 12 μL folding buffer (333 mM HEPES-KOH at pH 8, 20 mM $MgCl_2$, 333 mM NaCl) and incubated at 37°C for 20 min. To 9 μL (1 pmol) of the folded RNA, 1 μL of 130 mM NMIA (Molecular Probes) in anhydrous DMSO or 1 μL of anhydrous DMSO alone (control) was added and allowed to react at 37°C for 45 min (Wilkinson et al. 2006). The remaining 18 μL of folded RNA were divided into two aliquots (1 pmol RNA/tube) and stored on ice for sequencing.

Primer extension

To the NMIA-treated, DMSO control, or untreated RNA (1 pmol), 3 μL of a 0.3 μM 5′-[^{32}P] radiolabeled oligonucleotide (5′-^{32}P-GAACCGGACCGAAGCCCG or 5′-^{32}P-GCGTGTGGTC ATGAAAGTG, obtained from the Nucleic Acids Core Facility at the University of North Carolina at Chapel Hill) was added and the samples were incubated at 65°C for 5 min and then at 35°C for 20 min for primer annealing. To each reaction, 6 μL of reverse transcription buffer (250 mM KCl, 167 mM Tris-HCl at pH 8.3, 17 mM DTT, and 0.42 mM each dNTP) were added. For sequencing reactions using the untreated RNA, 2.5 μL of either 5 mM ddCTP or ddTTP were also added. After heating to 52°C, 1 μL (200 units) reverse transcriptase (Superscript III, In vitrogen) was added and the primer extension reaction was performed at 52°C for 3 min. Reactions were quenched with 1 μL of 4 M NaOH and heated at 95°C for 5 min. For gel analysis, 29 μL of a gel loading solution (40 mM Tris-borate, 5 mM EDTA, 276 mM unbuffered Tris-HCl, 0.01% [w/v] bromophenol blue and xylene cyanol and 73% [v/v] formamide) were added and the samples were heated at 95°C for an additional 5 min (Wilkinson et al. 2006).

Analysis

cDNA products from the (+) and (−) NMIA and sequencing reactions were separated by denaturing gel electrophoresis (10% polyacrylamide). Gels (21 cm × 40 cm × 0.4 mm) were subjected to electrophoresis at 1400 V for 1.5 or 4 h. Bands were quantified by phosphorimaging (Molecular Dynamics). Band intensities in the (+) and (−) NMIA lanes were quantified using SAFA (Das et al. 2005) and corrected for signal drop-off (Badorrek and Weeks 2006). Normalized SHAPE reactivities were calculated by subtracting intensities from the (−) NMIA control from the (+) NMIA reaction and divided by the average reactivity of the 8% most reactive positions. These reactivity values were then used as quasi-energetic constraints to constrain a thermodynamic folding algorithm, as implemented in RNAstructure (Mathews et al. 2004; K.E. Deigan, T.W. Li, D.H. Mathews, and K.M. Weeks, unpubl.). Stabilities for individual helices, as reported in Figures 2C, 3C, 4C, 5, and 6, were calculated without adding SHAPE reactivities.

ACKNOWLEDGMENTS

This work was supported by a grant from the United Mitochondrial Disease Foundation to L.L.S. and by NIH grants to L.L.S. (GM32734) and K.M.W. (GM56222).

Received November 7, 2007; accepted January 22, 2008.

REFERENCES

Anderson, S., Bankier, A.T., Barrell, B.G., de Bruijn, M.H.L., Coulson, A.R., Drouin, J., Eperon, I.C., Nierlich, D.P., Roe, B.A., Sanger, F., et al. 1981. Sequence and organization of the human mitochondrial genome. *Nature* **290:** 457–465.

Anderson, S., de Brujin, M., Coulson, A., Eperon, I., Sanger, F., and Young, I. 1982. Complete sequence of bovine mitochondrial DNA: Conserved features of the mammalian mitochondrial genome. *J. Mol. Biol.* **156:** 683–717.

Badorrek, C.S. and Weeks, K.M. 2006. Architecture of a γ retroviral genomic RNA dimer. *Biochemistry* **45:** 12664–12672.

Boni, I.V. 2006. Diverse molecular mechanisms for translation initiation in prokaryotes. *Mol. Biol. (Mosk.)* **40:** 658–668.

Das, R., Laederach, A., Pearlman, S.M., Herschlag, D., and Altman, R.B. 2005. SAFA: Semiautomated footprinting analysis software for high-throughput quantification of nucleic acid footprinting experiments. *RNA* **11:** 344–354.

Eddy, S.R. 2004. How do RNA folding algorithms work? *Nat. Biotechnol.* **22:** 1457–1458.

Gualerzi, C.O., Brandi, L., Caserta, E., Teana, A., Spurio, R., Tomsic, J., and Pon, C.L. (2000). Translation initiation in bacteria. In *The ribosome: Structure, function, antibiotics, and cellular interactions* (eds. R.A. Garrett et al.), pp. 477–494. ASM Press, Washington DC.

Hauswirth, W.W. and Laipis, P.J. 1982. Mitochondrial DNA polymorphism in a maternal lineage of holstein cows. *Proc. Natl. Acad. Sci.* **79:** 4686–4690.

Kapp, L.D. and Lorsch, J.R. 2004. The molecular mechanics of eukaryotic translation. *Annu. Rev. Biochem.* **73:** 657–704.

Koc, E.C. and Spremulli, L.L. 2002. Identification of mammalian mitochondrial translational initiation factor 3 and examination of its role in initiation complex formation with natural mRNAs. *J. Biol. Chem.* **277:** 35541–35549.

Liao, H.-X. and Spremulli, L.L. 1989. Interaction of bovine mitochondrial ribosomes with messenger RNA. *J. Biol. Chem.* **264:** 7518–7522.

Mathews, D.H. and Turner, D.H. 2006. Prediction of RNA secondary structure by free energy minimization. *Curr. Opin. Struct. Biol.* **16:** 270–278.

Mathews, D.H., Sabina, J., Zuker, M., and Turner, D.H. 1999. Expanded sequence dependence of thermodynamic parameters improves prediction of RNA secondary structure. *J. Mol. Biol.* **288:** 911–940.

Mathews, D.H., Disney, M.D., Childs, J.L., Schroeder, S.J., Zuker, M., and Turner, D.H. 2004. Incorporating chemical modification constraints into a dynamic programming algorithm for prediction of RNA secondary structure. *Proc. Natl. Acad. Sci.* **101:** 7287–7292.

Merino, E.J., Wilkinson, K.A., Coughlan, J.L., and Weeks, K.M. 2005. RNA structure analysis at single nucleotide resolution by selective 2′-hydroxyl acylation and primer extension (SHAPE). *J. Am. Chem. Soc.* **127:** 4223–4231.

Moll, I., Grill, S., Gualerzi, C.O., and Blasi, U. 2002. Leaderless mRNAs in bacteria: Surprises in ribosomal recruitment and translational control. *Mol. Microbiol.* **43:** 239–246.

Moll, I., Hirokawa, G., Kiel, M.C., Kaji, A., and Blasi, U. 2004. Translation initiation with 70S ribosomes: An alternative pathway for leaderless mRNAs. *Nucleic Acids Res.* **32:** 3354–3363. doi: 10.1093/nar/gkh663.

Montoya, J., Ojala, D., and Attardi, G. 1981. Distinctive features of the 5′-terminal sequences of the human mitochondrial mRNAs. *Nature* **290:** 465–470.

Nakamoto, T. 2006. A unified view of the initiation of protein synthesis. *Biochem. Biophys. Res. Commun.* **341:** 675–678.

Sachs, A., Sarnow, P., and Hentze, M.W. 1997. Starting at the beginning, middle, and end: Translation initiation in eukaryotes. *Cell* **89:** 831–838.

Sharma, M.R., Koc, E.C., Datta, P.P., Booth, T.M., Spremulli, L.L., and Agrawal, R.K. 2003. Structure of the mammalian mitochondrial ribosome reveals an expanded functional role for its component proteins. *Cell* **115:** 97–108.

Shine, J. and Dalgarno, L. 1974. The 3′-terminal sequence of *Escherichia coli* 16S ribosomal RNA: Complementarity to nonsense triplets and ribosome binding sites. *Proc. Natl. Acad. Sci.* **71:** 1342–1346.

Taanman, J.-W. 1999. The mitochondrial genome: Structure, transcription, translation, and replication. *Biochim. Biophys. Acta* **1410:** 103–123.

Udagawa, T., Shimizu, Y., and Ueda, T. 2004. Evidence for the translation initiation of leaderless mRNAs by the intact 70 S ribosome without its dissociation into subunits in eubacteria. *J. Biol. Chem.* **279:** 8539–8546.

Wilkinson, K.A., Merino, E.J., and Weeks, K.M. 2005. RNA SHAPE chemistry reveals non-hierarchical interactions dominate equilibrium structural transitions in $tRNA^{Asp}$ transcripts. *J. Am. Chem. Soc.* **127:** 4659–4667.

Wilkinson, K.A., Merino, E.J., and Weeks, K.M. 2006. Selective 2′-hydroxyl acylation analyzed by primer extension (SHAPE): Quantitative RNA structure analysis at single nucleotide resolution. *Nat. Protoc.* **1:** 1610–1616.

Zuker, M. 2003. Mfold web server for nucleic acid folding and hybridization prediction. *Nucleic Acids Res.* **31:** 3406–3415. doi: 10.1093/nar/gkg595.